Optimal control of a high efficiency low distortion 6-level hybrid multilevel motor drive

Sébastien Mariéthoz
Automatic Control Laboratory, ETH Zürich
Physikstrasse 3, CH - 8092 Zürich, Switzerland
Email: mariethoz@control.ee.ethz.ch

***Abstract*—The paper deals with optimal design and control of electric drives. A hybrid multilevel inverter drive structure is proposed in order to reduce converter switching losses and motor switching induced losses. Analysis demonstrates that low order harmonics may be generated by these type of converters when employing inappropriate control approaches. It proposes a control approach that features low tracking distortion over full range of operating points, during transients and inverter capacitor voltage imbalances, while minimizing switching losses. Proposed multilevel inverter control scheme is integrated into an MPC control scheme that optimally controls the drive.**

I. Introduction

Multilevel converters have been introduced in order to overcome silicon device voltage limits and reduce waveform distortion [1]–[4]. Hybrid multilevel inverters have been introduced in order to combine several complementary circuits in order to obtain better overall performance [5]–[8]. For some topologies, the hybridization is obtained by combining three-level H-bridge cells of different voltage ratings. These power converter structures feature a relatively large number of cells. As many isolated transformer windings as cells are required to provide the required isolated voltage sources, generally through rectifiers in order to reduce the overall complexity of the power supply. As a consequence these topologies are best suited for applications with no energy recovery.

Topologies combining a three-level inverter with three-level H-bridge cells have been introduced to diminish [6] or eliminate [7] the need for isolated power supplies. They are best suited for vehicle applications, where it is desired to recover energy during braking. Appropriately designed and controlled, they can feature increased energy efficiency and reduced harmonic distortion [6], which also results in reduced motor losses.

Several control strategies have been proposed in order to reduce the inverter switching losses. The difficulty is to control the inverter optimally over its full range of operation. Some previously proposed control strategies feature low switching losses but also some low harmonic distortion, especially at full magnitude, during transients or with capacitor voltage imbalances. For drive applications, it is necessary to operate the inverter over its full range of magnitudes with little distortion in order to obtain satisfactory control performance.

This paper proposes to use the topology introduced in [6] to design a high dynamic performance high energy efficiency multilevel drive (see Fig. 1). The objectives are to feature low switching losses, low conduction losses, close to zero motor ripple losses and high dynamic performance employing a sensorless control scheme. A strategy to avoid the low-frequency distortion introduced by the multilevel inverter operation is proposed. It allows satisfactory performance of the observers, which are particularly sensitive to inverter distortion.

II. Topology overview

A. Concepts

The drive topology is shown in Fig. 1. It is comprised of a "higher voltage cell", an IGBT three-phase two-level inverter connected in series with "lower voltage cells", three 3-level MOSFET H-bridge inverters. The properties that are relevant for the energy efficiency and harmonic distortion depend on the voltage ratio between the higher and lower voltage cells. They are described in [6] for three-phase inverters.

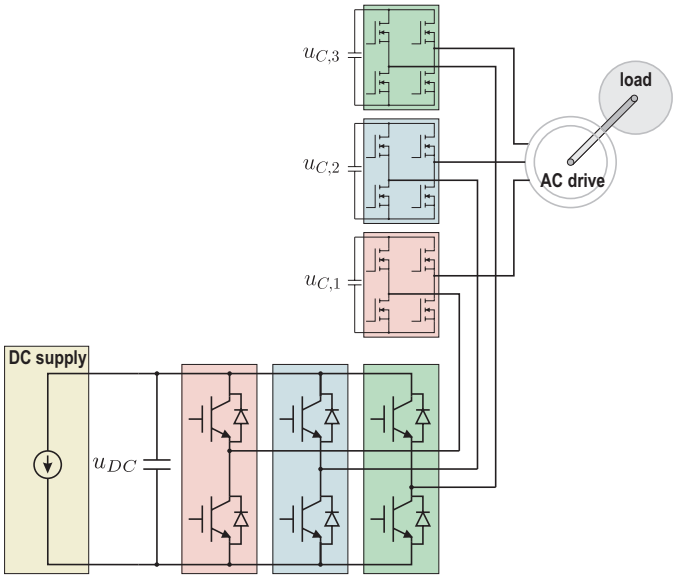

Fig. 1. Drive topology overview

1) Even space-vector distribution: An important property is to design an inverter that features an even distribution of the space vectors in order to feature the same low ripple magnitude over the full range of operation of the inverter: for this topology, the largest ratio that allows obtaining this space-vector uniformity property is 4. A very important property

978-1-4244-8218-4/10/$26.00 ©2010 IEEE

to design an inverter that features low switching losses is to be able to switch the higher voltage cell at the fundamental switching frequency.

2) Low switching losses: The ability of the hybrid inverter to be operated with low switching losses is measured by the concept of optimized modulation domain, which is the set that contains the reference space vectors that can be synthesized without switching the high voltage cell (featured by gray and cross hatched areas in Fig. 4(a)-(c)). The largest ratio that practically allows obtaining a compact optimized modulation domain (without holes) is 3 (example featured in Fig. 4).

3) Simple and efficient power supply: Another important property is to feature a power breakdown, such that most of the power flows from the higher voltage cell in order to reduce the power solicitation on the lower voltage cell [6]. This is obtained by having the largest voltage magnitude synthesized by the higher voltage cell, which suggests that the highest possible voltage ratio that allows switching the high-voltage cell at reduced switching frequency must be selected: 3 in the present case.

B. Semiconductor switches' selection

This section describes how to realize the topology of Fig. 1 with off-the-shelf silicon devices and motors. The maximum line-to-line voltage for this ratio is $u_{\max} = 5/3\,u_{DC} \approx 1.67\,u_{DC}$. In sine operation the phase voltage is about $0.96\,u_{DC}$. Two different switching devices of similar current ratings, with voltage ratings in the selected ratio have to be selected to optimally use the switching devices. To realize an AC drive that would feature the same voltage and current ratings as a conventional 2-level 3-phase with $600\,V$ at the DC-link ($230\,V$ RMS phase voltage) a combination of $600\,V$ IGBT with $200\,V$ DC-link or $250\,V$ MOSFET should be selected. The DC-link voltage would optimally be $u_{DC,\text{nom}} = 360\,V$ for the higher voltage cell and $u_{C,1,\text{nom}} = u_{C,2,\text{nom}} = u_{C,3,\text{nom}} = 120\,V$ for the lower voltage cells, yielding $245\,V$ maximum RMS phase voltage, which perfectly matches the application requirements. It has to be noted that these voltages can be slightly modified without significantly affecting the overall system performance.

III. Control System Overview

The control system comprises two cascade observers, a motor torque controller and a multilevel inverter controller (see Fig. 2). A standard MRAS structure is employed as flux and speed observer. A linear observer is employed to compensate delay and improve control scheme performance. The model predictive torque controller determines the inverter reference space-vector to be synthesized in order to optimize dynamic performance (optimal in the sense that it minimizes the tracking error through the control objective cost function. The inverter reference space-vector is employed to synthesize a PWM pattern that minimizes distortion and switching losses. The two latter parts are discussed in more details in the following sections.

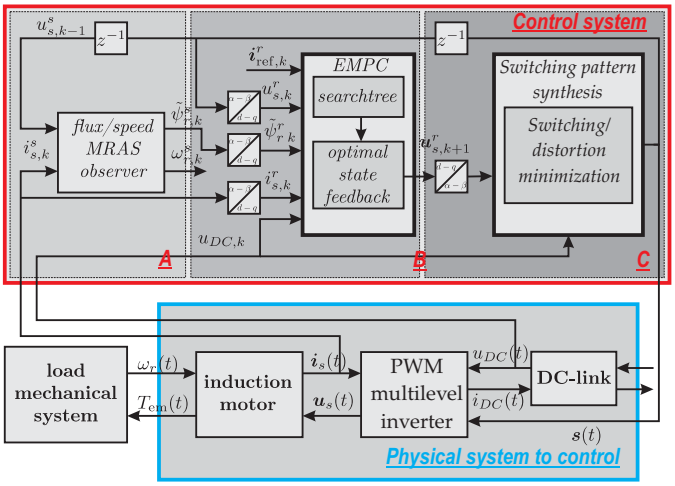

Fig. 2. Control system overview

IV. Motor Control

The model predictive torque control scheme proposed in [9] is suitable for multilevel drive. The control law is synthesized by computing the solution to a finite time constrained optimal control problem that is formulated by writing:

1) a cost function,
2) a model of the system dynamics,
3) a set of inequality constraints.

A. State and disturbance observer

The rotor flux is estimated through a MRAS observer. The state is defined employing the stator currents and rotor flux in rotor flux coordinates:

$$\hat{\boldsymbol{x}}_{k+1|k} = \begin{bmatrix} \hat{\boldsymbol{i}}_{s,k+1} \\ \hat{\boldsymbol{\psi}}_{r,k+1} \end{bmatrix} \tag{1}$$

A linear observer is employed in order to compensate the computational time delay by predicting the next state from the currently applied stator voltage:

$$\begin{aligned} \epsilon_k &= i_{s,k} - \boldsymbol{C}\hat{\boldsymbol{x}}_{k|k-1} \\ \hat{\boldsymbol{x}}_{k|k} &= \hat{\boldsymbol{x}}_{k|k-1} + \boldsymbol{L}_x\,\epsilon_k \\ \hat{\boldsymbol{w}}_{k|k} &= \hat{\boldsymbol{w}}_{k|k-1} + \boldsymbol{L}_w\,\epsilon_k \\ \hat{\boldsymbol{x}}_{k+1|k} &= \boldsymbol{A}_d\,\hat{\boldsymbol{x}}_{k|k} + \boldsymbol{B}_d\boldsymbol{u}_{s,k} + \hat{\boldsymbol{w}}_{k|k}. \end{aligned} \tag{2}$$

This observer also estimates a disturbance term, which accounts for model mismatch. This term reflects the parameter mismatch and the neglected terms that are due to the rotor and flux angular velocities. The feedback gains can be synthesized optimally using Kalman filter framework.

B. Constrained optimal control problem formulation

1) Cost function: The control objective is to minimize the tracking error between the target and the actual state over the

prediction horizon:

$$J = \sum_{n=1}^{N} \left(\boldsymbol{x}_{k+n|k} - \boldsymbol{x}_{\mathrm{tar},k}\right)^T \boldsymbol{Q} \left(\boldsymbol{x}_{k+n|k} - \boldsymbol{x}_{\mathrm{tar},k}\right) + \left(\boldsymbol{u}^r_{s,k+n-1} - \boldsymbol{u}_{s,\mathrm{tar},k}\right)^T \boldsymbol{R} \left(\boldsymbol{u}^r_{s,k+n-1} - \boldsymbol{u}_{s,\mathrm{tar},k}\right) \tag{3}$$

The cost function is selected to tailor the closed-loop system behaviour by capturing the control trade-offs through the matrix $\boldsymbol{Q}$ and $\boldsymbol{R}$.

2) Model equality constraints: The initial motor electrical state is obtained from observer (2):

$$\boldsymbol{x}_{k|k} = \hat{\boldsymbol{x}}_{k+1|k} \tag{4a}$$

The sequence of future states is predicted from the initial state using a model that features the time varying velocity dependent part of the motor dynamics as a disturbance term:

$$\boldsymbol{x}_{k+n+1|k} = \boldsymbol{A}_d\, \boldsymbol{x}_{k+n|k} + \boldsymbol{B}_d \boldsymbol{u}_{s,k+n} + \boldsymbol{w}_{k+n|k}. \tag{4b}$$

This model enters as a set of equality constraints in the optimal control problem. The role of these model depending constraints is to link the predicted states and manipulated control variables. The target is obtained by adding equality constraints that specify the relation between the target, the reference and the disturbance at steady state:

$$\begin{bmatrix} \boldsymbol{I} - \boldsymbol{A} & \boldsymbol{B} \\ \boldsymbol{C} & \boldsymbol{0} \end{bmatrix} \begin{bmatrix} \boldsymbol{x}_{\mathrm{tar},k} \\ \boldsymbol{u}_{\mathrm{tar},k} \end{bmatrix} = \begin{bmatrix} \boldsymbol{B}_w \\ \boldsymbol{I} \end{bmatrix} \begin{bmatrix} \boldsymbol{w}_k \\ \boldsymbol{y}_{\mathrm{ref},k} \end{bmatrix} \tag{4c}$$

The disturbance $\boldsymbol{w}_{k+n|k}$ is obtained from the same observer that allows obtaining the initial state (4a) (see [9]). Employing this formulation allows to ensure offset free torque and flux control (see [10] for existence and stability).

3) Inequality constraints: For the considered problem, the constraints are the maximum admissible current

$$\hat{i}_{s,d,k+n} < i_{\max,k} \tag{5a}$$

and the maximum available inverter voltage

$$\boldsymbol{H}_u \boldsymbol{u}^r_{s,k+n-1} \leq \boldsymbol{K}_u\, u_{DC,k} \tag{5b}$$

(5b) is a linear matrix inequality constraint that expresses the output voltage capability of the inverter, which is approximated by a polygon of radius $u_{DC,k}$ [11].

C. Explicit model predictive controller

The optimal stator voltages are found by solving the CFTOC problem defined by the cost function and the constraints formulated in (3)-(5) at each sampling instant. The corresponding optimization problem is a quadratic program (QP). The optimal solution is a piecewise affine map between the initial state and the stator voltages that can be computed off-line [12] on the form:

$$\boldsymbol{u}^r_{s,k+n-1} = \begin{cases} \boldsymbol{K}_1\, \boldsymbol{x}_{k|k} & \text{when} \quad \boldsymbol{H}_1\, \boldsymbol{x}_{k|k} \preceq \boldsymbol{0} \\ \boldsymbol{K}_2\, \boldsymbol{x}_{k|k} & \text{when} \quad \boldsymbol{H}_2\, \boldsymbol{x}_{k|k} \preceq \boldsymbol{0} \\ \vdots & \vdots \quad\quad \vdots \\ \boldsymbol{K}_R\, \boldsymbol{x}_{k|k} & \text{when} \quad \boldsymbol{H}_R\, \boldsymbol{x}_{k|k} \preceq \boldsymbol{0} \end{cases} \tag{6}$$

The CFTOC problem (3)-(5) is formulated using Yalmip high level optimization language under Matlab [13]. The associated QP is solved parametrically using the multi-parametric toolbox (MPT) [14] yielding the control law (6). The number of regions R depends on the number of inequality constraints and on the length of the prediction horizon. It is about 100 for the proposed control scheme. (6) can be effectively computed by running a binary search tree where an affine function is evaluated at each node [15].

V. Multilevel pulse width modulation

The explicit model predictive torque controller (6) computes the optimal average stator voltage that must be applied to the motor at each sampling period. The role of the multilevel pulse width modulator is to generate a voltage pattern that produces an effect as close as possible to this optimal average stator voltage by modulating the inverter available voltage levels. Different modulation strategies may be employed to reach different objectives in terms of obtained voltage and flux distortions, required number of inverter transitions and scheme complexity. In this work, digital asymmetrical triangular carrier technique is employed as it is simple and allows obtaining very low distortion both for the voltage and flux for three-phase systems [16].

VI. Multilevel inverter control

The modulator provides an *ideal* pattern defined by space vectors and time intervals to be applied by the inverter. Due to the space vector redundancies, there are several *similar* ways of synthesizing the chosen voltage pattern, that lead to *ideally identical* line-to-line voltage profile. These different ways of generating the same voltage pattern are however not equivalent from the point of view of the converter losses. The role of the inverter control strategy is to select the voltage pattern in a sensible way that allows minimizing the losses or optimizing some other objective. Due to the unavoidable imbalance between the cell voltages, the the time intervals for which the feasible space vectors have to be applied need to be readjusted to reduce low frequency distortion. It may sometime not be possible to provide sufficient stator voltage with the selected pattern. It may therefore sometime be advised to rearrange the pattern obtained by the pulse width modulator in order to reach the desired voltage or reduce switching losses. The latter however seriously increases the scheme complexity for a marginal benefit.

A. Control approaches for reduced switching losses

Several different strategies may be considered to reduce the converter switching losses.

1) Synergetic approach: In this approach, a transition level is employed to take decisions when to switch the large voltage cell [17]. This approach naturally features low switching losses at steady state. The transition level can be adjusted in order to adjust the power flow between the cells. This allows to employ rectifiers to supply the low voltage cells [5] with some restrictions.

The approach is however not optimal during transients: it can yield excessive switching losses during operation around the transition level.

2) State-space optimal approach: In [18], an optimal state machine is built from the state space representation to yield optimal switching.

The limit of this approach is that the state machine becomes large and more difficult to build for 3-phase inverters with many levels.

3) Minimum switching strategy: The synergetic approach can be extended to deal with space vectors and to avoid excessive switching during transients, as described in [6].

The strategy can be framed as follows. The value of the large voltage cell currently applied space vector $u'_{A,k}$ needs to be stored as state variable. At each sampling instant, one checks if the lower voltage cell contribution $u'_{a,k}$ can be sufficient to allow reaching the reference from the stored high voltage cell state. $u_{A,k}$ is not switching as long as $u'_{a,k}$ is sufficient to reach reference as illustrated in Fig. 3(a). When it is not anymore the case, as illustrated in Fig. 3(b), it is then necessary to switch the large voltage cell to reach the reference. A transition of the higher voltage cell to a new switching state from which the low voltage cell contribution is sufficient is required. A way to maximize the chance the reference is reachable from the new selected higher voltage cell switching state is to select the high voltage cell space vector that is the closest to the reference as illustrated in Fig. 3(c). This approach ensures minimum switching losses.

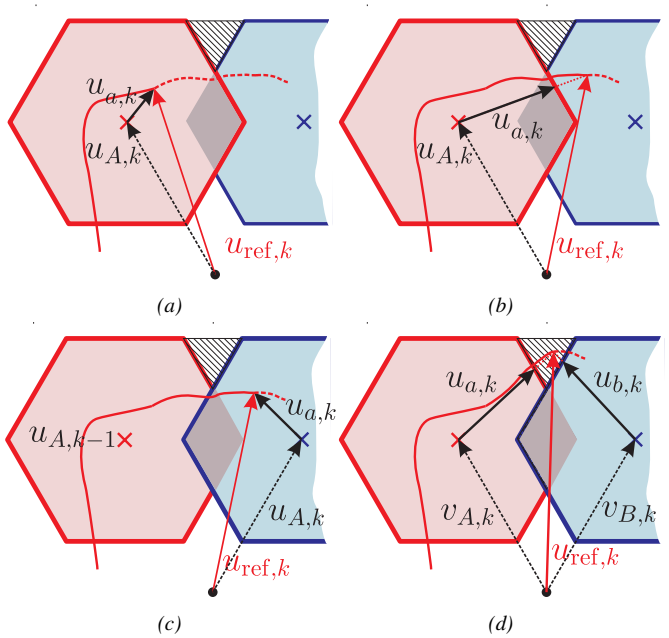

Fig. 3. (a) Reference is reachable by $u_{a,k}$ without switching $v_{A,k}$. (b) Reference is not reachable without switching $v_{A,k}$. (c) $v_{A,k}$ is switched to reach reference. (d) Reference cannot be reached employing this strategy.

The limit of this approach is that the space vectors that do not belong to the optimized modulation domain (see hatched areas in Fig. 4(a)) are not directly reachable employing the described approach. The space vectors out of the optimized modulation domain are not feasible without modulating the higher voltage cell, as illustrated in Fig. 3(d). Different clipping strategies can be applied to obtain a feasible voltage pattern that reduces the resulting distortion. The present strategy instead selects the closest space vectors that can be synthesized without modulating the higher voltage cell: see how sine reference of Fig. 4(b) is truncated in Fig. 4(c) and the resulting distortion represented in time domain on Fig. 4(d). This distortion obviously reduces the control quality.

B. Proposed minimum switching and distortion strategy

The only way to synthesize a vector in the hatched areas of Fig. 4(a) is to generate a PWM switching pattern that includes switching of the higher voltage cell (modulation of the space vector $u_{A,k}$ and $u_{B,k}$ in Fig. 5(a)). Doing this switching at the PWM frequency increases the losses for the maximum magnitude trajectories that cross these areas, which significantly increases the overall losses. Furthermore, this high frequency switching may not be feasible if the switches of the high voltage cell are too slow.

The proposed strategy to avoid the mentioned drawbacks is stated as follows. When exiting the optimized modulation domain, a reduced magnitude vector is applied for several switching periods by saturating the low voltage cell, represented by the combination of the vectors $v_{A,k} + v_{a,k}$. The error $\epsilon_{a,k}$ that is caused by the saturation is integrated:

$$\epsilon_{a,k} = u_{\mathrm{ref},k} - v_{A,k} - v_{a,k} \tag{7a}$$

$$\Sigma_{a,k+1} = \Sigma_{a,k} + \epsilon_{a,k} \tag{7b}$$

When the reference enters again in the optimized modulation domain, the integrated error is compensated by applying a correction in the other direction, represented by the combination of the vectors $v_{B,k} + v_{b,k}$ such that:

$$v_{B,k} + v_{b,k} + \Sigma_{a,k} - u_{\mathrm{ref},k} = 0 \tag{8}$$

If the reference, remains out of the optimized modulation domain for more than a given number of switching periods, determining the minimum admissible switching period for the high voltage cell, then the same correction procedure is applied by switching the high voltage cell. The resulting current and flux ripples are increased but this scheme considerably reduces the low frequency distortion, while maintaining the switching frequency of the high voltage cell low thus ensuring low overall losses.

One has to ensure that the correction can be obtained in one switching period in order to minimize the distortion. This means that the correction vector has to belong to the optimized modulation domain. The first condition to ensure the correction is feasible is to maintain the switching period of the high voltage cell below some value. There are several way of clipping the low voltage cell reference that affect the feasibility of the correction. A simple way of ensuring the correction is always feasible is to always generate a vector of the similar module as the reference vector, such that correction

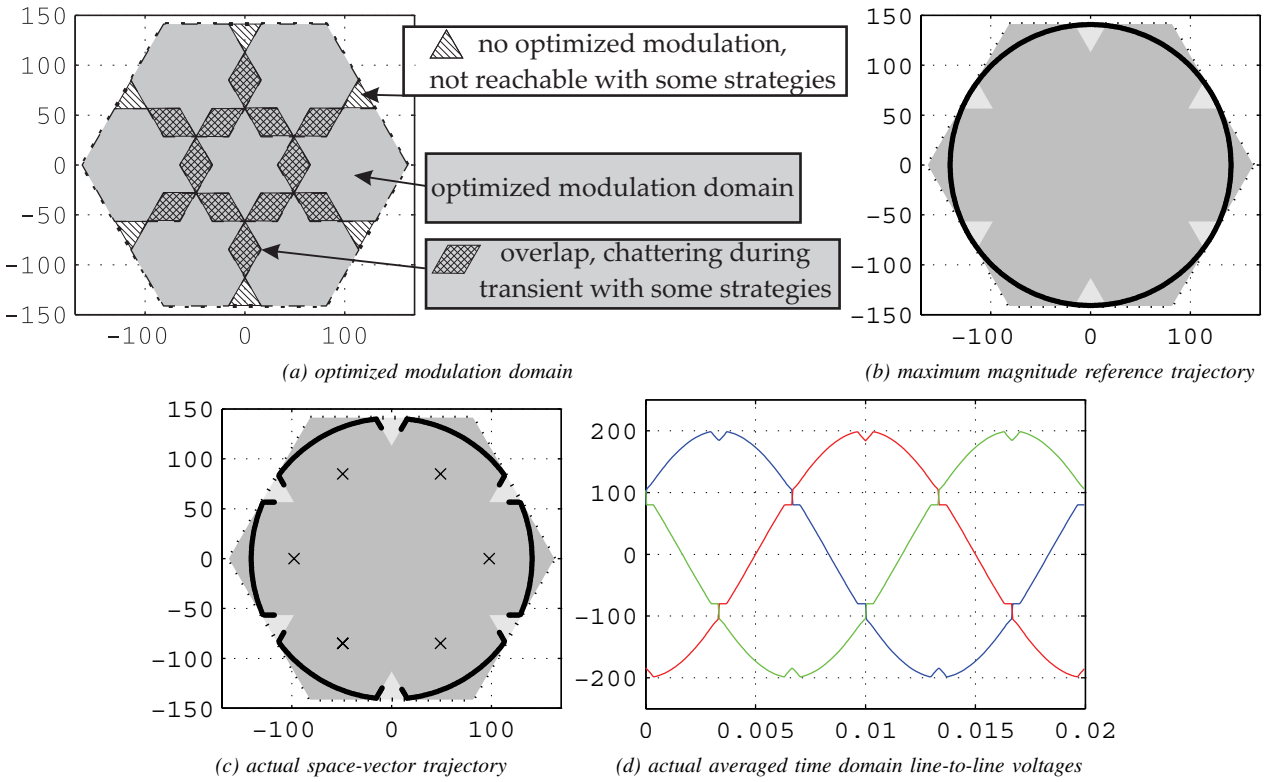

Fig. 4. Applying optimal modulation strategy for reduced switching losses V.A.3, some high magnitude space vectors are not in the optimized modulation domain and thus not accessible, resulting in truncated trajectory of (c) and low frequency distortion visible in (d).

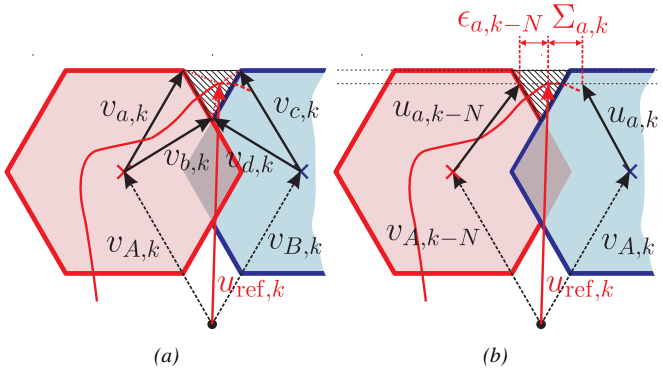

Fig. 5. To reduce harmonic distortion it is necessary to (a) modulated the high voltage cell or (b) correct the distortion at a slower switching frequency

in phase only is required, not in magnitude. This means that the reference is clipped along the axis that is parallel to the outer bound reachable by the inverter as shown in Fig. 5(b). This also allows to have a simple correction procedure.

VII. Experimental results

The proposed multilevel inverter drive was build and control scheme was validated on a 750 W drive system that comprises two coupled motors. The complete control scheme is implemented on a 32-bit 40 MHz floating point DSP, which demonstrate its practical feasibility. Initial experimental measurements are shown in Fig. 6 for a fast start-up transient for the induction motor. DC-link voltage is one third of the nominal voltage for this test, such that full inverter magnitude is reached at 32 Hz electrical frequency. It can be seen that the line-to-line voltage features 11 levels at full magnitude (see Fig. 6(g)), dynamic performance is very good and little distortion is observed on the currents (Fig. 6(f) and (h)), which confirms effectiveness of the proposed strategy. The higher voltage cell switches only at fundamental switching frequency as shown in Fig. 6(c), while the lower voltage cells improve the voltage quality (see Fig. 6(d)) switching one third of the DC-link voltage at $4\,kHz$.

VIII. Conclusion

A drive system has been proposed that features reduced switching losses and ripple. It has been shown that state-of-the-art control strategies for reduced switching losses cause low harmonic distortion for large magnitude voltage required to operate the drive at high speed with nominal torque. A strategy has been proposed to modify the inverter control and modulation strategies in order to eliminate these low order harmonics while retaining the converter low switching loss feature. High dynamic performance can be obtained by employing an model predictive control scheme. Experimental results confirm that high dynamic performance and current quality can be obtained while featuring low switching losses.

References

[1] A. Nabae and H. Akagi. A new neutral-point-clamped PWM inverter. *IEEE Trans. on Ind. Applicat.*, 17(5):518–523, September 1981.

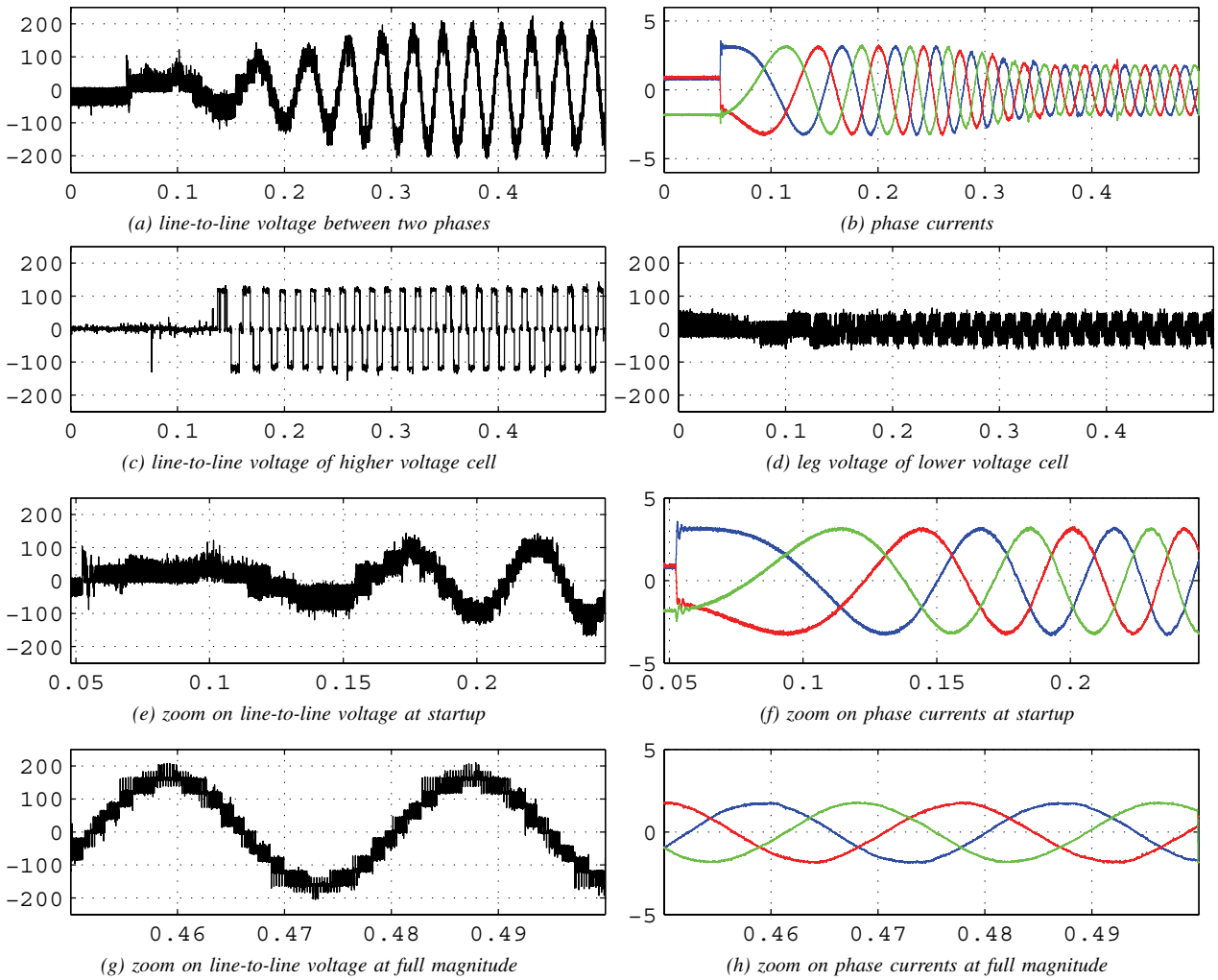

(a) line-to-line voltage between two phases

(b) phase currents

(c) line-to-line voltage of higher voltage cell

(d) leg voltage of lower voltage cell

(e) zoom on line-to-line voltage at startup

(f) zoom on phase currents at startup

(g) zoom on line-to-line voltage at full magnitude

(h) zoom on phase currents at full magnitude

Fig. 6. Experimental validation of the proposed control strategy with a startup test. Magnetization followed by a 80 % torque step producing an acceleration from 0 to 32 Hz. DC supply voltage is 120 V such that full inverter magnitude is reached at reduced speed: (a) (e) (g) line-to-line voltage features 11 levels at full magnitude, (b) (f) (h) dynamic performance is very good and little distortion is observed on the currents, (c) higher voltage cell switches at reduced frequency (d) lower voltage cells reduce ripple.

[2] M. Marchesoni, M. Mazzucchelli, and S. Tenconi. A non conventional power converter for plasma stabilization. In *Proc. Power El. Spec. Conf.*, volume 1, pages 122–129, 1988.

[3] T. Meynard and H. Foch. Multi-level choppers for high voltage applications. *EPE Journal*, 2(1):45–50, 1992.

[4] L. Delmas, T. Meynard, H. Foch, and G. Gateau. Smc : Stacked multicell converter. In *Proc. Power Conversion and Motion Conf. (PCIM)*, volume 43, pages 63–69, May 2001.

[5] M.D. Manjrekar, P.K. Steimer, and T.A. Lipo. Hybrid multilevel power conversion system: A competitive solution for high-power applications. *IEEE Trans. on Ind. Applicat.*, 36(3):834–841, May 2000.

[6] S. Mariethoz and A. Rufer. New configurations for the three-phase asymmetrical multilevel inverter. In *Proc. IEEE Ind. Applicat. Conf.*, Nov. 2004.

[7] M. Veenstra and A. Rufer. Control of a hybrid asymmetric multilevel inverter for competitive medium-voltage industrial drives. *IEEE Trans. on Ind. Applicat.*, 41(2):655–664, Mar. 2005.

[8] T. Chaudhuri, P. Steimer, and A. Rufer. The common cross connected stage for the 5L ANPC medium voltage multilevel inverter. *IEEE Trans. on Ind. El.*, 57(Forthcoming), 2010.

[9] S. Mariéthoz, A. Domahidi, and M. Morari. High dynamic performance constrained optimal control of induction motors. In *Proc. Applied Power Electronics Conf., APEC*, Palmsprings, Ca, USA, Feb. 2010.

[10] U. Mäder, F. Borrelli, and M. Morari. Linear offset-free model predictive control. *Automatica*, 45(10):2214 – 2222, 2009.

[11] S. Mariéthoz, A. Domahidi, and M. Morari. Sensorless Explicit Model Predictive Control of Permanent Magnet Synchronous Motors. In *Proc. IEEE Int. El. Machine and Drive Conf. (IEMDC)*, May 2009.

[12] A. Bemporad, F. Borrelli, and M. Morari. Model Predictive Control Based on Linear Programming - The Explicit Solution. *IEEE Trans. on Aut. Control*, 47(12):1974–1985, Dec. 2002.

[13] J. Löfberg. YALMIP : A Toolbox for Modeling and Optimization in MATLAB. In *Proc. of the CACSD Conf.*, Taipei, Taiwan, 2004.

[14] M. Kvasnica, P. Grieder, and M. Baotić. Multi-Parametric Toolbox (MPT), 2004.

[15] P. Tondel, T.A. Johansen, and A. Bemporad. Computation and approximation of piecewise affine control laws via binary search trees. In *Proc. of the 41st IEEE Conf. on Decision and Control*, volume 3, pages 3144 – 3149, Dec 2002.

[16] S. Mariethoz and A. Rufer. A new single-phase multilevel modulator - a fast and accurate method to compute the modulator harmonic spectra. In *Proc. European Power Elec. and Motion Control Conf.*, Sep. 2004.

[17] C. Rech and J.R. Pinheiro. Hybrid multilevel converters: Unified analysis and design considerations. *IEEE Trans. on Ind. El.*, 54(2):1092 – 1104, Apr. 2007.

[18] S. Mariethoz and A.C. Rufer. Design and control of asymmetrical multilevel inverters. In *Proc. IEEE Ind. El. Conf.*, volume 1, pages 840–845, November 2002.